

Ferromagnet proximity effects and magnetoresistance of bilayer graphene

Y. G. Semenov and K. W. Kim

*Department of Electrical and Computer Engineering,
North Carolina State University, Raleigh, NC 27695-7911*

J. M. Zavada

U.S. Army Research Office, Research Triangle Park, NC 27709

Abstract

A drastic modification of electronic band structure is predicted in bilayer graphene when it is placed between two ferromagnetic insulators. Due to the exchange interaction with the proximate ferromagnet, the electronic energy dispersion in the graphene channel strongly depends on the magnetization orientation of two ferromagnetic layers, \mathbf{M}_1 and \mathbf{M}_2 . While the parallel configuration $\mathbf{M}_1 = \mathbf{M}_2$ leads to simple spin splitting of both conduction and valence bands, an energy gap is induced as soon as the angle θ between \mathbf{M}_1 and \mathbf{M}_2 becomes non-zero with the maximum achieved at $\theta = \pi$ (i.e., antiparallel alignment). Consequently, bilayer graphene may exhibit a sizable magnetoresistive effect in the current-in-plane configuration. A rough estimate suggests the resistance changes on the order of tens of percent at room temperature. This effect is expected to become more pronounced as the temperatures decreases.

PACS numbers: 73.21.-b,85.75.-d,73.43.Qt,73.61.Wp

With the advent of the creation of free-standing atomically thin graphite films (or graphene) [1], a lot of unusual electronic properties related with two-dimension Dirac-like relativistic spectrum of the honeycomb carbon lattice [2] put graphene in the forefront of emerging carbon based electronics. Among other the half-integer quantum Hall effect [3, 4, 5], which was observed at room temperature [6], the high carrier mobility in wide range of temperatures, the easy controlling of the electron and hole concentration under by variation of applied bias, absence of weak localization and universal minimal conductivity at the Dirac point with zero density of states, etc, attracted a huge theoretical and experimental attention to transport properties of graphene during past two years [7, 8].

Spin properties of graphene monolayer have also received much attention. The starting point for the most of such consideration is the extremely small spin-orbital coupling in graphene compared to common semiconductors [9]. Owing to this, graphene exhibits long electronic mean paths [10, 11] even at room temperature [12] and long electron spin-relaxation time [13]. Graphene might also be a material for the realization of spin qubits and quantum computing due to low hyperfine interaction of the localized electron spin with the ^{13}C carbon isotope [14]. However, the weak spin-orbital interaction presents a severe challenge in spin manipulation or selection during electron transmission through the graphene channel. One possible approach may be to utilizes the electron exchange interaction with a proximate dielectric ferromagnet for the control of spin rotation [15] or the spin-dependent potential [16].

It was found very recently that bilayer graphene (BLG) offers a host of novel phenomena through external modification of the energy band structure [17, 18, 19, 20, 21, 22]. Particularly, it was shown that a gap opens up between the conduction and valence energy bands when a difference u is introduced in the site potentials of the graphene layers. Moreover, the parabolic band structure of the non-equivalent K and K' valleys at $u = 0$ [23] transforms to a Mexican-hat-like dispersion with energy chink $u > 0$ at centrum valleys and slightly reduced gap $\tilde{u} < u$ at a distance from the K and K' points [18, 19]. These results may also point to non-trivial response on symmetry braking of spin-dependent interaction in GBL.

In this work we study the electronic structure of BLG sandwiched in between isolating/dielectric ferromagnets with non-equal magnetic moments \mathbf{M}_1 and \mathbf{M}_2 . The modification of electronic band structure is caused by the exchange interaction of each graphene layer with its proximate magnets. The remarkable peculiarity of such system appears for

identical ferromagnets with equal magnetic moments, $M_1 = M_2$, so that $u = 0$ and *potential asymmetry* does not modify band structure. However in the case of disalignment between \mathbf{M}_1 and \mathbf{M}_2 the spin interactions reveal asymmetry with respect to both magnets that can modify the graphene energy bands. Apparently, in the case of monolayer graphene, the total effect of two magnets reduces to the electron spin splitting in the effective field induced by the vectorial sum $\mathbf{M}_1 + \mathbf{M}_2$.

The structure we consider illustrates schematically Fig. 1. It resembles the ferromagnet-metal hybrid structures [24, 25, 26] that reveals a giant magnetoresistance owing to spin-dependent conductivity [27, 28]. The bottom ferromagnetic dielectric layer (FDL) possesses the magnetization \mathbf{M}_1 which can be pinned along the direction of x axis by antiferromagnetic substrate. The top FDL is constructed from the same material but its magnetization vector \mathbf{M}_2 may possess an arbitral direction in the $x-y$ plane formatting the angle θ with \mathbf{M}_1 . The influence of FDL magnetization on BLG electronic structure becomes apparent through the exchange interaction, which assumes some overlap between carbon π -orbitals and non-filling shells of the magnetic ions in FDLs or indirect interaction with magnetic ions through the ligands of FDLs. Such interaction is actual between nearest graphene layer and FDL, thus, in mean field approximation, the problem can be modeling with Hamiltonian

$$H = H_{BL} + \mathcal{P}_1 \alpha \mathbf{M}_1 \mathbf{S} + \mathcal{P}_2 \alpha \mathbf{M}_2 \mathbf{S}, \quad (1)$$

where H_{BL} is a spin-independent BLG Hamiltonian, the rest part of the Eq. (1) describes the energy of an electron spin \mathbf{S} in the effective fields (in energy units) $\alpha \mathbf{M}_1$ and $\alpha \mathbf{M}_2$ of the proximate FDLs. Projection operator $\mathcal{P}_1 = 1$ for electron localized at the bottom carbon monolayer and $\mathcal{P}_1 = 0$ for the upper carbon monolayer; correspondingly $\mathcal{P}_2 = 0$ and 1. Parameter α is proportional to the carrier-ion exchange constants and has been evaluated in Refs. 15, 16.

We are interested in the low energy electron excitations. Previous theoretical analysis of this problem was performed in terms of the tight-binding approximation [18, 19] and the density functional theory [21], which actually confirmed the approximation of Refs. 18, 19 in the case of low energy electronic excitations. We use the tight-binding Hamiltonian near the centers of valleys in a basis that constitutes the components $(A_1 \uparrow, A_1 \downarrow, B_2 \uparrow, B_2 \downarrow, A_2 \uparrow, A_2 \downarrow, B_1 \uparrow, B_1 \downarrow)$ for the K valley and $(B_2 \uparrow, B_2 \downarrow, A_1 \uparrow, A_1 \downarrow, B_1 \uparrow, B_1 \downarrow, A_2 \uparrow, A_2 \downarrow)$ for the K' valley, where \uparrow and \downarrow denote electron states with spin up and spin down. A_i and

B_i corresponds to electron amplitudes at inequivalent sites of the bottom ($i = 1$) and top ($i = 2$) layers.

The Hamiltonian H_{BL} includes the lateral coupling for nearest carbon atoms in bottom, $A_1 - B_1$, and top $A_2 - B_2$ layers with matrix element $\gamma = 3$ eV, and interlayer coupling for $A_2 - B_1$ and $A_1 - B_2$ dimers with matrix element $\gamma_1 = 0.4$ eV and $\gamma_3 = 0.3$ eV respectively (i.e., $\gamma_3 < \gamma_1 \ll \gamma$) (Fig.1). At zero magnetic field the Eq. (1) can be expressed in terms of the in-plane electron momentum $\mathbf{k} = \{k_x, k_y\}$ so that in tight-binding approximation [18, 19], the lowest electronic states in the K and K' valleys describe the Hamiltonian

$$H_{\varkappa} = \varkappa \begin{pmatrix} -\frac{1}{2}u & \frac{\varkappa}{2}\alpha M_{\varkappa} & v_3 k e^{i\varphi} & 0 & 0 & 0 & v k e^{-i\varphi} & 0 \\ \frac{\varkappa}{2}\alpha M_{\varkappa}^* & -\frac{1}{2}u & 0 & v_3 k e^{i\varphi} & 0 & 0 & 0 & v k e^{-i\varphi} \\ v_3 k e^{-i\varphi} & 0 & \frac{1}{2}u & \frac{\varkappa}{2}\alpha M_{-\varkappa} & v k e^{i\varphi} & 0 & 0 & 0 \\ 0 & v_3 k e^{-i\varphi} & \frac{\varkappa}{2}\alpha M_{-\varkappa}^* & \frac{1}{2}u & 0 & v k e^{i\varphi} & 0 & 0 \\ 0 & 0 & v k e^{-i\varphi} & 0 & \frac{1}{2}u & \frac{\varkappa}{2}\alpha M_{-\varkappa} & \varkappa \gamma_1 & 0 \\ 0 & 0 & 0 & v k e^{-i\varphi} & \frac{\varkappa}{2}\alpha M_{-\varkappa}^* & \frac{1}{2}u & 0 & \varkappa \gamma_1 \\ v k e^{i\varphi} & 0 & 0 & 0 & \varkappa \gamma_1 & 0 & -\frac{1}{2}u & \frac{\varkappa}{2}\alpha M_{\varkappa} \\ 0 & v k e^{i\varphi} & 0 & 0 & 0 & \varkappa \gamma_1 & \frac{\varkappa}{2}\alpha M_{\varkappa}^* & -\frac{1}{2}u \end{pmatrix}, \quad (2)$$

where the index \varkappa separates the case of K ($\varkappa = +1$) and K' ($\varkappa = -1$) valley. In Eq. (2) we introduce $\varphi = \text{Arctan}(k_y/k_x)$, and $M_{+1} = M_1$, $M_{-1} = M_2 e^{-i\theta}$. $v = \sqrt{3}a\gamma/2\hbar$ is an electron velocity at the Fermi energy in graphene monolayer [3], the term with velocity $v_3 = \sqrt{3}a\gamma_3/2\hbar \ll v$ is responsible for trigonal warping, where $a = 0.249$ nm is a length of lattice unit vector.

We are looking for the solution of the secular equation with the matrix Eq. (2) assuming (i) zero bias, and (ii) the identical top and bottom FM materials ($M_1 = M_2 \equiv M$, $u = 0$). For simplicity sake, we ignore the transfer matrix elements for off-center sites A_1 and B_2 ($v_3 \rightarrow 0$). The last simplification does not change qualitatively the results for the energies $E > 1$ meV [22] that assumes to be justly.

At the specified conditions, the energy spectrum in each valley consists in eight non-degenerated branches $\varepsilon_n(p)$ identical for conduction and valence bands and symmetrical with respect to valley centrum (i.e., independent on φ). Two spin pairs of them corresponds to the excited branches with energies $|\varepsilon_n(p)| \gtrsim \gamma_1$, which are beyond the our interest; the rest four spin bands $\varepsilon_n = \varepsilon_n(k)$ describe the low energy electronic spectrum. Hereinafter it is convenient to apply energy parameters in units of γ_1 introducing dimensionless momentum

$p = vk/\gamma_1$ and exchange field $\mathbf{G} = \alpha\mathbf{M}/\gamma_1$, which is actually a small parameter, $G < 1$. Thus, the low energy electron excitations $\varepsilon_n = \pm\gamma_1 E_\pm$ can be expressed in the angle range $0 \leq \theta \leq \pi$ as

$$E_\pm^2 = p^2 + \frac{G^2}{4} + \frac{1}{2} \left(1 \pm G \cos \frac{\theta}{2} - W_\pm \right), \quad (3)$$

where

$$W_\pm = \sqrt{\left(1 \pm G \cos \frac{\theta}{2} \right)^2 (1 + 4p^2) + 2p^2 G^2 (1 - \cos \theta)}. \quad (4)$$

Two solutions with $E_\pm > 0$ corresponds to bottom of spin-split conduction bands while symmetrical (with respect to zero energy) bands $E_\pm < 0$ describe the top of valence band. The energy spectrum possesses a fixed chink $\Delta E_0 = G$ in centrum of each valley at $p = 0$. Figure 2 exhibits the low energy spectrum modification related to the rotation of the top FDL magnetization with respect to bottom one.

The most remarkable result consists in gradual opening the energy gap E_g with \mathbf{M}_2 rotation under fixed \mathbf{M}_1 so that in the case of $\theta = 0$ [i.e. $\mathbf{G}_1 = \mathbf{G}_2$, Fig. 2(a)] the net effect of spin splitting leads to $E_g = 0$ at contact point $p = \sqrt{G(1 + G/2)/2}$ while the case $\theta = \pi$ [i.e. $\mathbf{G}_1 = -\mathbf{G}_2$, Fig. 2(d)] remains the spin-degeneration of electronic states with maximal $E_g = G/\sqrt{1 + G^2}$ at $p = G\sqrt{2 + G^2}/2\sqrt{1 + G^2}$. The spin degeneracy at $\theta = \pi$ is not surprising because graphene layer equivalency makes both \mathbf{G}_1 and $\mathbf{G}_2 = -\mathbf{G}_1$ directions indistinguishable [i.e., the dependence of Eqs. (3) and (4) on sign in $\pm G$ disappears]. Note that in the case of monolayer graphene, the effect of two FDL in similar configuration $\mathbf{G}_2 = -\mathbf{G}_1$ gives rise to quenching of any spin-dependent modifications of the band structure.

In the case of arbitrary disalignment the bandgap describe the expression

$$E_g = \frac{G \sin \theta/2}{\sqrt{1 + G^2 + 2G \cos \theta/2}}. \quad (5)$$

As is evident from the Eq. (5) the strength of the effective field G determines the amplitude of the E_g variation. If its magnitude is comparable with thermal energy $k_B T$ (in units of γ_1) the dependence (5) may manifest itself through the variation of electron/hole population with \mathbf{M}_2 rotation, or magnetoresistance, which assume the sensitivity of \mathbf{M}_2 direction to relatively weak external magnetic field \mathbf{B} . Figure 2 also demonstrates the flattening effect in the conduction/valence bands with increasing θ that should enhance the effect of magnetoresistance $R(\mathbf{B})$ or $R(\theta)$.

The effect of both carriers populations and bands flattening on the $R(\theta)$ can be taken into account in one-electron approximation in terms of Kubo-Greenwood formula for conductivity [29, 30]

$$\sigma_{xx} = (2\pi e)^2 \hbar \sum_{m,n} \sum_{\mathbf{k},\mathbf{k}'} |\langle m, \mathbf{k} | v_x | n, \mathbf{k}' \rangle|^2 \left(-\frac{\partial f}{\partial \varepsilon} \right)_{m,\mathbf{k}} \delta(\varepsilon_{m,\mathbf{k}} - \varepsilon_{n,\mathbf{k}'}), \quad (6)$$

involving the electron charge e , the indices of spin subbands m and n , which are thermally populated by electrons/hols, the velocity operator $v_x = dx/dt = i[H_{\mathbf{x}}, x]/\hbar$, and Fermi function f . We analysis the case of ballistic conductivity at finite temperature [31]. The interest arouses the relative alteration of $\sigma_{xx}(\theta)/\sigma_{xx}(0)$ with angle θ changing. Analysis shows that $\sigma_{xx}(\theta)/\sigma_{xx}(0)$ is most sensitive to a single parameter $G/k_B T$, while it is proof against to G variation in wide range $G < 1$. Calculated variation of $\sigma_{xx}(\theta)$ with the help of Eq. (6) and its comparison with correspondent changing of the electron/hole concentration presents the Fig. 3. Relatively weaker decreasing of the carrier population as a function of θ demonstrates a significant contribution of the mobility variations due to flatter band structure.

Thus assuming the sensitivity of the \mathbf{M}_2 to the external magnetic field applied along the \mathbf{M}_1 (i.e., the x axis, see Fig. 1) one can define the magnetoresistance as a difference of the BLG resistance $R(0) \sim 1/\sigma_{xx}(0)$ at $\mathbf{M}_1 = \mathbf{M}_2$ and $R(\pi) \sim 1/\sigma_{xx}(\pi)$ at $\mathbf{M}_1 = -\mathbf{M}_2$. At the same time, the MR has to be sensitive to the electro-chemical potential μ so that the maximal effect is expected for $\mu = 0$. Figure 4 presents the calculations of the MR normalized on initial value $R(0)$, $\xi = [R(\pi) - R(0)]/R(0)$, as a function of $G/k_B T$ under few fixed values $|\mu|/k_B T$. It is important to note that a realization of the exchange field strength $G \approx 0.04$ eV may be of practical interest because it leads to $\xi \approx 60\%$ at room temperature. By comparison, the alternative approach based on spin-valve devices with graphene monolayer as a connection of ferromagnetic leads reveals a feeble magnetoresistance because of weak dependence of the graphene conductivity on the electronic details of the leads [32].

As a practical matter, the strength of the exchange field G plays a crucial significance. However, taking into account a huge number of possible realizations of the FDL/graphene interfaces, the evaluation of G *a priori* may be done in very rough manner. Following to the approach presented in the Ref.[16] we estimate the exchange energy for graphene electron interacting with nearest stratum of the magnetic ions with areal concentration n_{2FM} and areal concentration of carbon atoms n_{2C} by the expression $G = (n_{2FM}/n_{2C})SJ$, where S

is a mean value of the magnetic ion spins and J is the exchange constant. The latter was found to be $J = 15$ meV as deduced from experiment for the structure EuO/Al with Curie temperature $T_c = 69$ K.[33] One might expect that in the case of high temperature ferromagnets with stronger spin-spin inter-ions interaction, the constant J may be larger. With the provision that $J \sim T_c$, $n_{2FM}/n_{2C} = 0.1 \div 0.2$, $S = 1 \div 2.5$ and $T_c = 500 \div 600$ K we find $G = 0.015 \div 0.065$ eV. The provided estimation of the exchange energy is very rough so the magnitude of G should be taken rather from experiment. However it shows the potentialities of room temperature manifestation of evident magnetoresistance.

In summary, a modification of the electronic band structure of the BLG owing to the exchange interaction with proximate dielectric ferromagnets has considered. The effect is caused by inequality of the exchange fields for each proximate ferromagnets. Disalignment of identical ferromagnet magnetizations leads to gradual opening of bandgap that is accompanied by a flattening dispersion law in bottom (top) of conduction (valence) band. Both these features contribute to the magnetoresistance, which amounts to huge magnitude at low enough temperatures.

This work was supported in part by the US Army Research Office and the FCRP Center on Functional Engineered Nano Architectonics.

-
- [1] K. S. Novoselov¹, A. K. Geim, S. V. Morozov, Y. Zhang, S. V. Dubonos, I. V. Grigorieva, and A. A. Firsov, *Science* **306**, 666 (2004).
- [2] G. W. Semenoff, *Phys. Rev. Lett.* **53**, 2449 (1984).
- [3] K. S. Novoselov¹, A. K. Geim, S. V. Morozov, D. Jiang, M. I. Katsnelson, I. V. Grigorieva, S. V. Dubonos, and A. A. Firsov, *Nature (London)* **438**, 197 (2005).
- [4] Y. Zhang, Y.-W. Tan, H. L. Stormer, and P. Kim, *Nature (London)* **438**, 201 (2005).
- [5] V. P. Gusynon, S. G. Sharapov, *Phys. Rev. Lett.* **95**, 146801 (2005).
- [6] K. S. Novoselov¹, Y. Zhang, A. K. Geim, Y. Zhang, S. V. Morozov, H. L. Stormer, U. Zeittler, J. C. Maan, G. S. Boebinger, P. Kim, and A. K. Geim, *Science* **315**, 1379 (2007).
- [7] A. K. Geim and K. S. Novoselov, *Nature Mat.* **6**, 183 (2007).
- [8] V. I. Fal'ko, and A. K. Geim, *Eur. Phys. J.* **148**, 1 (2007).
- [9] H. Min, J. E. Hill, N. A. Sinitsyn, B. R. Sahu, L. Kleinman, and A. H. MacDonald, *Phys. Rev. B* **74**, 165310 (2006).
- [10] B. Oezylmaz and P. Kim, in *Final Program of the 2007 Electronic Materials Conference* (South Bend, Indiana, 2007), Vol. 1, p. 85.
- [11] S. Cho, Y.-Fu Chen, and M. S. Fuhrer, *Appl. Phys. Lett.* **91**, 123105 (2007).
- [12] N. Tombros¹, C. Jozsa, M. Popinciuc, H. T. Jonkman, and B. J. van Wees, *Nature (London)* **488**, 571 (2007).
- [13] D. Huertas-Hernando, F. Guinea, and A. Brataas, *Eur. Phys. J.* **148**, 177 (2007).
- [14] B. Trauzettel, D.V. Bulaev, D. LOSS, and G. Burkard, *Nature Phys.* **3**, 192 (2007).
- [15] Y. G. Semenov, K. W. Kim, J. Zavada, *Appl. Phys. Lett.* **91**, 153105 (2007).
- [16] H. Haugen, D. Huertas-Hernando, and A. Brataas, arXiv:cond-mat/0707.3976.
- [17] K. S. Novoselov, E. McCann, S. V. Morozov, V. I. Fal'ko, M. I. Katsnelson, U. Zeitler, D. Jiang, F. Schedin, and A. K. Geim, *Nature Phys.* **2**, 177 (2006).
- [18] E. McCann and V.I. Fal'ko, *Phys. Rev. Lett.* **96**, 086805 (2006).
- [19] E. McCann, *Phys. Rev. B* **74**, 161403 (2006).
- [20] E. V. Castro, K. S. Novoselov, S. V. Morozov, N. M. R. Peres, J. M. B. Lopes dos Santos, J. Nilsson, F. Guinea, A. K. Geim, and A. H. Castro Neto, arXiv:cond-mat/0611342.
- [21] H. Min, B. Sahu, S. K. Banerjee, and A. H. McDonald, *Phys. Rev. B* **75**, 155115 (2007).

- [22] E. McCann, D. S. L. Abergel, and V.I. Fal'ko, *Eur. Phys. J.* **148**, 91 (2007).
- [23] M. S. Dresselhouse and D. Dresselhouse, *Adv. Phys.* **51**, 1 (2002).
- [24] M. N. Baibich, J. M. Broto, A. Fert, F. N. V. Dau, F. Petroff, P. Eitenne, G. Creuzet, A. Frederich, and J. Chazelas, *Phys. Rev. Lett.* **61**, 2472 (1988).
- [25] G. Binasch, P. Grünberg, F. Saurenbach, and W. Zinn, *Phys. Rev. B* **39**, R4828 (1989).
- [26] S. S. P. Parkin, N. More, and K. P. Roche, *Phys. Rev. Lett.* **64**, 2304 (1990).
- [27] See, for example, *Spin Electronics*, ed. D. Awschalom (Kluwer, Dordrecht, 2004).
- [28] S. A. Wolf, A. Y. Chtchelkanova, and D. M. Treger, *IBM J. Res. Dev.* **50**, 101 (2006).
- [29] R. Kubo, *J. Phys. Soc. Japan* **12**, 570 (1957).
- [30] D. A. Greenwood, *Proc. Phys. Soc.* **71**, 585 (1958).
- [31] The conductance of the graphene subjected to random potential was evaluated in terms of Kubo-Greenwood formula by K. Nomura, M Koshino, and S. Ryu, *Phys. Rev. Lett.* **99**, 146806 (2007).
- [32] L. Brey and H. A. Fertig, *Phys. Rev. B* **76**, 205435 (2007).
- [33] G. M. Roesler, M. E. Filipkowski, P. R. Broussard, Y. U.Idzerda, M. S. Osofsky, and R. J. Soulen, *Proc. SPIE* **2157**, 285 (1994).

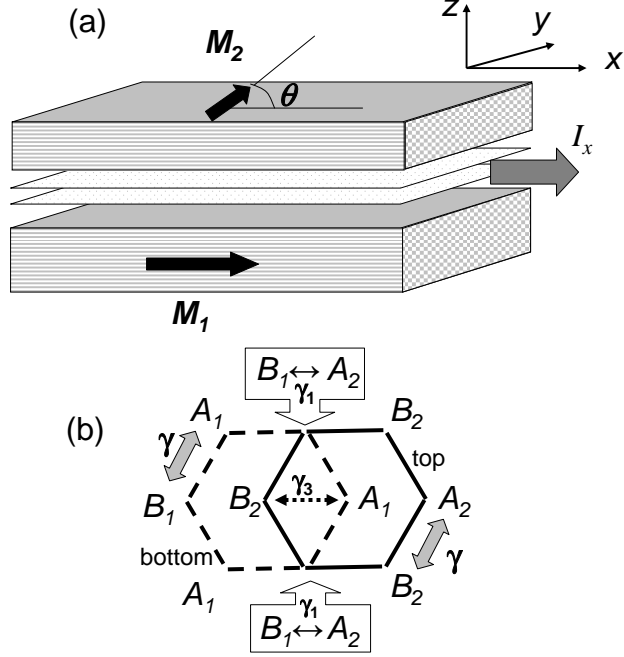


FIG. 1: (a) Schematic illustration of the bilayer graphene (two closely set planes) clamped between ferromagnetic dielectric layers possessing different magnetizations \mathbf{M}_1 and \mathbf{M}_2 (black arrows); θ is the angle between \mathbf{M}_1 and \mathbf{M}_2 . The reference frame is chosen so that \mathbf{M}_1 is directed along x axis; Grey arrow shows the probing current I_x through the graphene channel. (b) Fragment of the bilayer graphene (view from above) as the two hexagons with carbon atoms located at their vertexes. Lattice sites A_1 and B_1 (dashed hexagon) refer to the bottom layer while A_2 and B_2 (solid hexagon) refer to the top one. The double-sided grey arrows, single boxed arrow and double-sided dashed one display the actual electron transfer between in-plane nearest carbons (matrix element γ), vertical (γ_1) and slanting (γ_3) inter-layer transfer correspondingly.

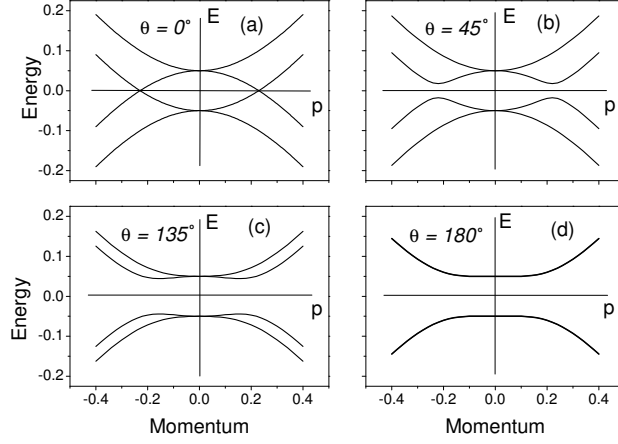


FIG. 2: Electron energy spectrum of bilayer graphene at different angles θ of disalignment between magnetization vectors \mathbf{M}_1 and \mathbf{M}_2 . Zero energy $E = 0$ corresponds to center of bandgap [(b) - (d)] and a point of contact of conduction and valence bands in the case $\theta = 0$ (a). Thick line in the graph (d) exhibits the double degeneracy of the spectrum at $\theta = \pi$.

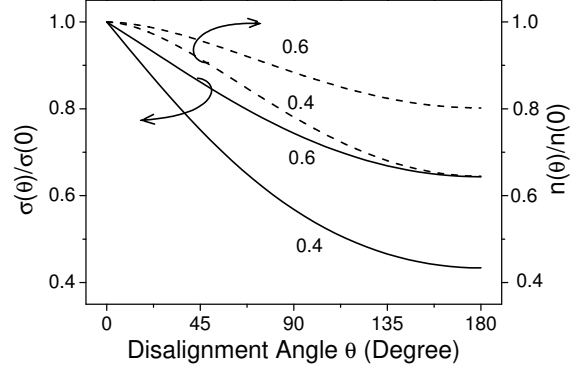


FIG. 3: Conductivity $\sigma(\theta)$ (solid lines) and carrier concentration $n(\theta)$ (dashed lines) alteration with disalignment angle θ in bilayer graphene at different ratios of the thermal energy $k_B T$ to exchange field $\gamma_1 G$. The magnitude $k_B T / \gamma_1 G$ is depicted at each curve. Electro-chemical potential is fixed at zero.

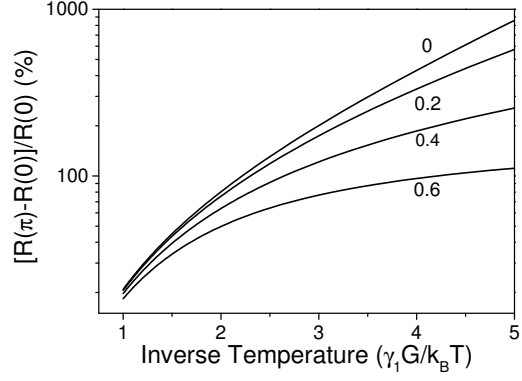


FIG. 4: Magnetoresistance associated with the magnetization \mathbf{M}_2 flip in an external magnetic field under the fixed \mathbf{M}_1 (Fig. 1) as a function of ratio of the exchange field strength $\gamma_1 G$ to thermal energy $k_B T$ calculated at different levels of electro-chemical potential μ . The ratios $\mu/k_B T$ are depicted at each curve.